

Damage Identification of a Concrete Arch Beam Based on Frequency Response Functions and Artificial Neural Networks

V.V. Nguyen, U. Dackermann, J. Li & M. Makki Alamdari

The Centre for Built Infrastructure Research, University of Technology, Sydney, Sydney, Australia

S. Mustapha

Department of Mechanical Engineering, American University of Beirut, Beirut, Lebanon

Infrastructure, Transport and Logistics, National ICT of Australia, Sydney, Australia

P. Runcie

Infrastructure, Transport and Logistics, National ICT of Australia, Sydney, Australia

L. Ye

Centre for Advanced Materials Technology, The University of Sydney, Sydney, Australia

Email: Van.V.Nguyen-1@student.uts.edu.au

ABSTRACT: This paper presents a vibration-based structural health monitoring (SHM) technique for the identification of damage in a concrete arch beam replica section of the Sydney Harbour Bridge. The proposed technique uses residual frequency response functions (FRFs) combined with principal component analysis (PCA) to form a damage specific feature (DSF) that is used as an input parameter to artificial neural networks (ANNs). Extensive laboratory testing and numerical modelling are undertaken to validate the method. In the proposed technique, FRFs are obtained by the standard modal testing and damage is identified using ANNs that innovatively map the DSF to the severity of damage (length of damage cut). The results of the experimental and numerical validation show that the proposed technique can successfully quantify damage induced to a concrete arch beam simulating a real life structural component of the Sydney Harbour Bridge.

Keywords: *Structural health monitoring, Damage detection, Sydney Harbour Bridge, Frequency response functions, Artificial neural network, Non-destructive testing, Principal component analysis*

1 INTRODUCTION

A critical mission for structural health monitoring (SHM) of bridges is to provide a reliable assessment technique to potential hazards caused by structural damage or other structural defects using continuously monitored vibration data. Recognising the needs and shortcomings of SHM, a project was established by the National ICT of Australia (NICTA), the University of Technology, Sydney (UTS) and The University of Sydney to develop reliable damage detection methods to provide robust and accurate assessment techniques for critical bridge infrastructure in Australia, in particular for the Sydney Harbour Bridge. In collaboration with the Road and Maritime Services (RMS) in NSW, a large number of accelerometers are installed on the Sydney Harbour Bridge to implement a SHM system that can continuously monitor the performance of the bridge's critical structural components and ensure the safety and reliability of Sydney's iconic structure. Particular attention is given to this structure since it has been in operation for over 80 years (Highway Engineering Australia 2012). This is of crucial importance since steel bridges are subject to a large number of repetitive loads over the course of their life mostly by passing vehicles, making it vul-

nerable to fatigue-related damage and failure (Ye et al. 2012).

The installed SHM system on the Sydney Harbour Bridge is aimed at providing a robust and reliable warning and evaluation system on the structural deficiencies of a series of jack arch beam-type components. One of the most critical issues in this study is focused on how to reliably detect and evaluate structural damage or deficiencies from continuous real-time monitored data of the bridge components under ambient vibration conditions. Recent studies have shown that the vibration measurements in SHM systems are subject to noise, and hence, make it more difficult to assess the condition of the structure. Magalhães, Cunha and Caetano (2012) have shown that the dynamic features of a structure are sensitive to changes in environmental conditions. The results of their study demonstrated that an increase in temperature will lower the first natural frequency of the structure. In addition to environmental sensitivity, evaluation of the bridge's loading capacity based on the estimated bridge condition also needs to be incorporated.

The on-going project of implementing a SHM system in the Sydney Harbour Bridge is currently in its first stage focusing on exploring the effectiveness and efficiency of various damage detection algorithms through numerical modelling to generate a

large number of damage cases and experimental investigations to validate the numerical model. The initial focus is on the jack arch beams supporting the bus lane.

The concept of using vibration response for damage detection SHM is desirable due to the practicality of using low cost sensors to continuously measure the dynamic response of the structure and the measureable effect that damage has on its vibration. A great deal of vibration-based damage detection research has focused on using modal parameters such as modal frequencies, modal damping and mode shapes, and their derivatives to form damage specific features (DSF). Among the three modal parameters, the modal frequency is the simplest DSF for detecting damage. According to Koh and Dyke (2006), changes in modal parameters, such as variances in frequencies and mode shapes, can be effective indicators for damage detection. Koh and Dyke (2006) demonstrated on a simple cantilever model that it is possible to determine the extent and location of a crack by applying the Multiple Damage Location Assurance Criterion (MDLAC) using the first five natural frequencies. Dyke et al. (2003) investigated the application of the same procedure to more complex models, such as an entire bridge structure, and found that at least 28 modal frequencies are required for the procedure to be effective. This, however, is unrealistic for SHM since ambient excitations are only capable of exciting a few lower modal frequencies of a bridge. In addition to this, low frequencies of the structure are more sensitive to environmental changes rather than changes caused by local damage. Modal shapes and their derivatives are found to be more sensitive to local damage. However, experimental modal analysis (EMA) is needed to extract modal shapes from measured experimental data and is a complicated and error prone process, which often requires human judgement from the operators.

Research undertaken in recent years has primarily focused on using directly measured data such as frequency response function (FRF) to assess the condition of a structure and to identify damage (Bandara et al. 2014). In comparison to processed data such as modal parameters, direct measurements from numerical and experimental modal testing have the advantage of retaining an abundance of information of a structure's dynamic behaviour from measured data as well as avoidance of labour intensive EMA. Thereby, operational human induced errors can be eliminated and crucial damage sensitive information is preserved. Furthermore, using direct measurements from real-time can make these methods favourable for online continuous monitoring.

One of the critical issues with developed damage detection algorithms is the reliability and robustness of the methods. The primary sources of difficulties

include measurement noise, modelling error, uncertainty of ambient conditions and incompleteness of measured data. An important aspect of damage identification research is therefore the discrimination of abnormal response variation due to damage from normal response variation caused by measurement noise, fluctuations of ambient conditions or operating uncertainty. Artificial neural networks (ANNs), a form of artificial intelligence, have strong abilities to learn from experience, generalize from examples, and identify underlying information from noisy data. In the presented method, the joint use of directly measured FRF data and a hierarchical system of ANNs (network ensembles) is therefore employed. Such approach has already been applied by some researchers and some successful results have been obtained (Zang and Imregun 2001; Ni et al. 2006; Li et al. 2009; Dackermann et al. 2013). In previous research, Principal Component Analysis (PCA) was used for data compression to address the issue of utilising large FRF data, which can cause problems in training convergence and computational efficiency in neural networks. PCA is a statistical technique that is known for its capability in reducing the dimensions of data as well as its ability to reduce the influence of uncertainties by filtering unrepeatable random features. Previous research investigated the capability of using the ANN model to detect damage from data obtained using the same experimental configuration and damage scenario as the data that was collected to train the ANN model. This paper will take this approach one step further by exploring the ANNs capabilities of testing measurements from damage cases that were not used to train the ANN model. As such, some generated damage cases will be used to train the ANN model and the remaining damage cases will be used for testing.

2 PROPOSED DAMAGE IDENTIFICATION APPROACH

In the proposed damaged identification method, an impact hammer is used to induce vibration to the test structure. In the presented study, the structure is a concrete arch beam specimen, which is a replica of one of many jack-arch cantilever beams that support the bus lane on the Sydney Harbour Bridge. The vibration response of the structure is captured using 15 accelerometers. From these acceleration measurements, the FRFs are derived forming the basis for the damage specific feature (DSF) utilised in this method. The aim is to use the DSF to train ANNs to estimate the severity of damage based on data derived from the acceleration measurements. A baseline is defined by the FRFs of the healthy structure. By subtracting the FRFs of the undamaged structure,

residual FRFs are generated emphasising the difference between the undamaged and the damage cases.

A major limitation with this approach is that the size of the residual FRFs is very large, making it impractical for ANN training. Data compression techniques are considered to rectify this issue. PCA is used to significantly reduce the data size by projecting its most important features to different principal components. The schematic of the proposed methodology is shown in Figure 1.

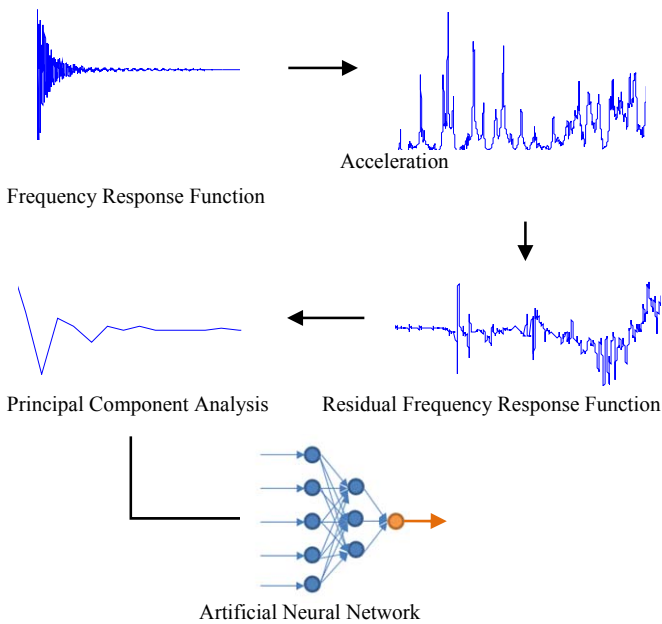


Figure 1. Schematic of damage identification method.

3 EXPERIMENTAL SETUP

The bus lane on the Sydney Harbour Bridge is supported by a series of connected arch type cantilever joints as shown in Figure 2a. For the experimental validation of the proposed damage identification method, a concrete specimen was produced that replicates the geometry and material properties of a single arch joint. The specimen comprised of 32 MPa characteristic strength concrete encasing a 200UB18 steel I-Beam with 50 mm concrete cover on both ends and had a length of 2 m. 15 accelerometers (PCB 352C34) were installed on the specimen to measure the vibration response resulting from impact excitation. The cross-section of the beam and the location of the accelerometers are shown in Figure 2b (A1 to A10 on front surface, A11 to A15 set back 300 mm). The National Instruments data acquisition system PXIe-4492 was used to record the data. The impact was applied 50 mm from the front and 50 mm from the right face of the specimen to excite vertical bending and torsional modes (see Figure 2c). 200 hammer strikes were executed and the structural response was recorded with a sampling

rate of 8 kHz over a period of two seconds for each impact.

After testing the structure in its healthy state, damage was inflicted to the specimen using a saw blade introducing a cut between accelerometer 2 and 3 as indicated in Figure 2b. The cut had a depth of 55 mm and was induced in four incremental stages each representing a different cut length. The structure was tested again after each damage stage. In total, five different structural conditions were tested:

- Healthy State: No damage
- Damage Case 1: Light damage with a cut length of 75 mm
- Damage Case 2: Medium damage with a cut length of 150 mm
- Damage Case 3: Severe damage with a cut length of 225 mm
- Damage Case 4: Extra severe damage with a cut length of 270 mm

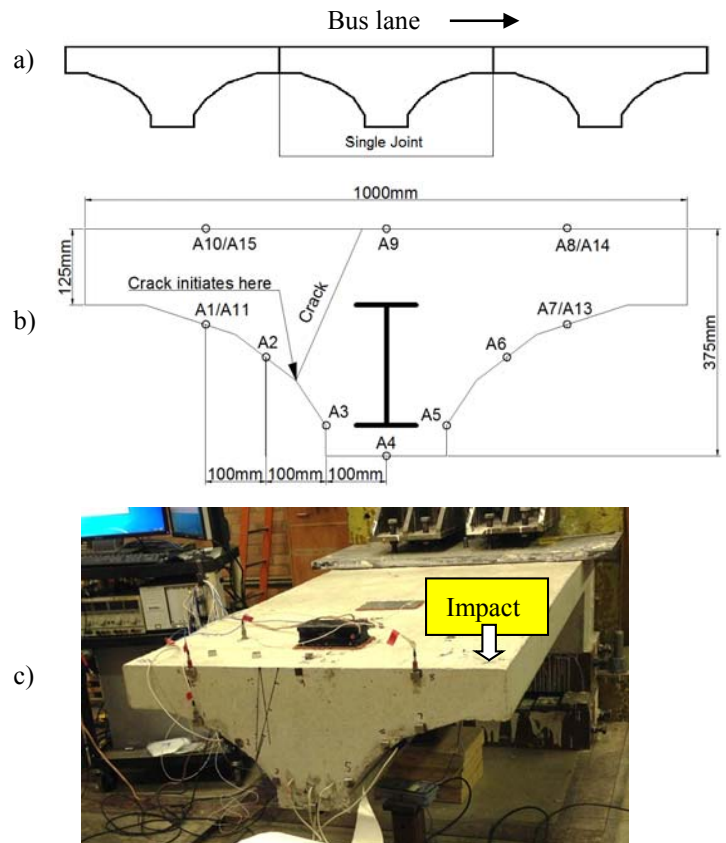


Figure 2. a) Series of arch type cantilever joints supporting the bus lane, b) dimensions of the experimental replica single joint specimen and accelerometer locations, c) experimental setup.

4 DAMAGE IDENTIFICATION PROCEDURE

4.1 Residual Frequency Response Functions

In the proposed damage identification procedure, the residual FRF data is processed to obtain unique

DSF. Residual FRFs emphasise the difference between FRF measurements of the structure in its healthy state and its damaged state. It can be calculated using Equation 1.

$$\text{Residual FRF} = \text{FRF}_{\text{undamaged}} - \text{FRF}_{\text{damaged}} \quad (1)$$

An example of FRFs from a single accelerometer is shown in Figure 3a. The FRFs of all impacts of the healthy case and all damage cases are averaged respectively. As it can be seen, the introduced damage has only a small effect on the FRFs making it difficult to distinguish between the healthy case and the damaged cases. It is therefore beneficial to obtain the differences between the FRFs of the damaged cases and the baseline FRF to emphasise the changes in the FRF caused by the damage. The residual FRF captures these changes and are shown in Figure 3b.

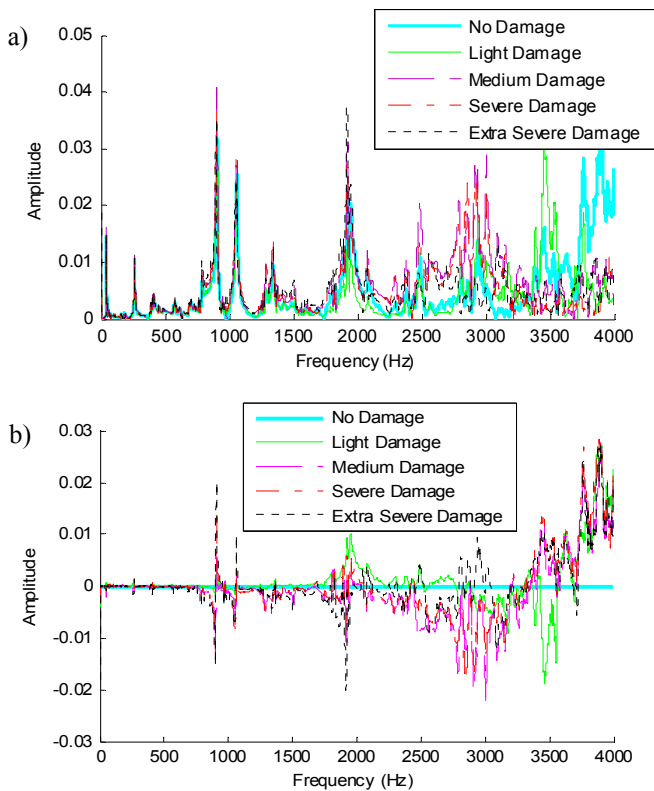


Figure 3. (a) FRFs of healthy case and all four damage cases (of a single accelerometer), and (b) residual FRFs of all four damage cases (of a single accelerometer).

4.2 Outlier Removal

Due to various factors, such as background noise and human errors, the acceleration measurements are subjected to uncertainties and do therefore include outliers. Utilising all recorded data, including the outliers, would result in ANNs being trained with poor quality data and hence would deliver poor quality results. To remove the outliers, in this study, the empirical rule is considered, which states that 99.73% of all data values lie within three standard

deviations of the mean of the data, assuming that the data has a normal distribution. This concept is illustrated in Figure 4.

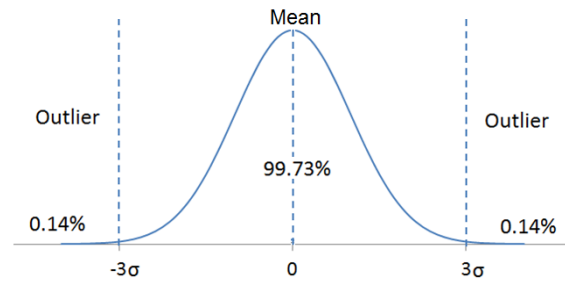


Figure 4. 3 Sigma normal distribution.

One of the challenges in applying this theory to the experimental data is that the residual FRF of each impact excitation (from a total of 200 excitations) consists of 4000 data points (for a frequency range from 0 to 2000 Hz) rather than a single value. In many cases, only a few of the data points were considered outliers and removing the sample based on only a small amount of outlier data points would result in excessive removal of data. This issue was overcome by defining a threshold of maximum number of data points that were outside of the three sigma boundary, and by classifying the data sets that exceeded this threshold as outlier data set. Table 1 lists the outlier count for accelerometers 1 to 5 for five impact excitations of the healthy state.

Table 1. Outlier count for accelerometers A1 to A15 for five impacts.

	A1	A2	A3	A4	A5	A6 – A15	Avg
Impact 1	24	42	22	109	0	...	66
Impact 2	234	282	242	248	79	...	184
Impact 3	0	0	0	0	0	...	0.2
Impact 4	0	8	19	0	0	...	2
Impact 5	14	21	30	24	14	...	18

From the example in Table 1, it can be seen that for impact excitation 2, there are a notable number of outliers across all fifteen accelerometers. This is a clear indicator that this impact is an outlier. Similarly, there are a notable number of outliers across most of the accelerometers of the first impact, marking this impact as an outlier. In contrast to this, there are also a number of outliers for the fifth impact excitation, however, this impact excitation is not considered to be an outlier in this analysis. In this case, the average number of outliers across the 15 accelerometers is only 18 out of the 4000 data points, which presents 0.45% of the data points. Figure 5 illustrates the outlier count for 30 impacts of the undamaged case. It can be seen that the outlier count is consistently high for all accelerometers of impact 2,

20, 22 and 24, which were classified as outlier data sets and subsequently removed.

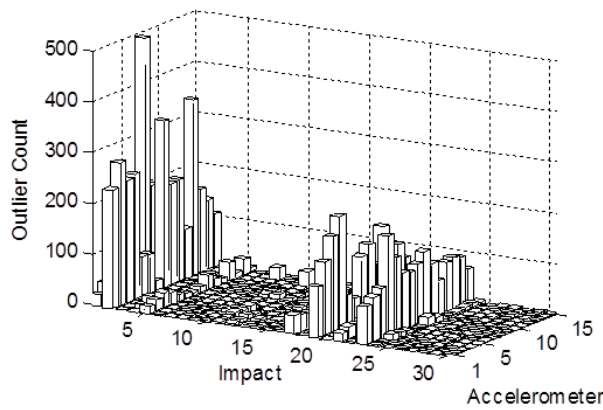


Figure 5. Outlier count identification.

To ensure that good quality data was maintained and used to train the ANNs, an outlier removal system was developed that removes impact data sets of an average outlier count above a certain threshold, which was defined to retain 150 of the 200 impact samples. For the case presented above, a threshold of 22.3 was defined as the threshold. 50 impact excitations had an average outlier count of over 22.3, hence 150 samples were retained.

Figure 6a and 6b show the residual FRFs of a single accelerometer before and after the outlier analysis. It can clearly be seen that the FRFs are much clearer after the outlier analysis. This process was repeated for all damage cases.

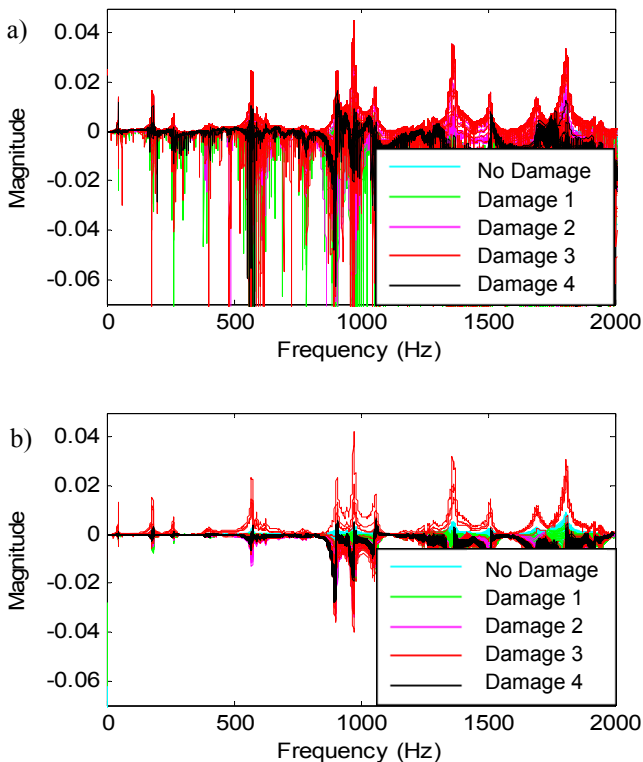


Figure 6. Removal of outliers in the frequency response functions. a) FRFs before outlier analysis, and b) FRFs after outlier analysis (for a frequency range from 0 to 2000 Hz).

4.3 Principal Component Analysis

PCA can overcome issues associated with using large-size data in ANNs and are capable of reducing measurement noise and other uncertainties. PCA is a statistical technique that projects data onto its most important principal components (PC), and thereby, it greatly reduces its size without significantly affecting the data. Eigenvalue decomposition of the covariance matrix forms the basis of PCA.

In the presented study, PCA is applied to the standard score of the linearly transform residual FRFs to compress the data to a smaller set of uncorrelated values. A standard score value for each data point is found by applying Equation 2 where x is the measured data point, μ is the mean value and σ is the standard deviation of the data points.

$$z - score = \frac{x - \mu}{\sigma} \quad (2)$$

In the resulting data, the first PC, which is the largest eigenvalue, represents the direction and amount of maximum variability of the residual FRF. The subsequent PCs have lower contribution to the data. The contributions of the derived PCs from one of the accelerometers are depicted in Figure 7a.

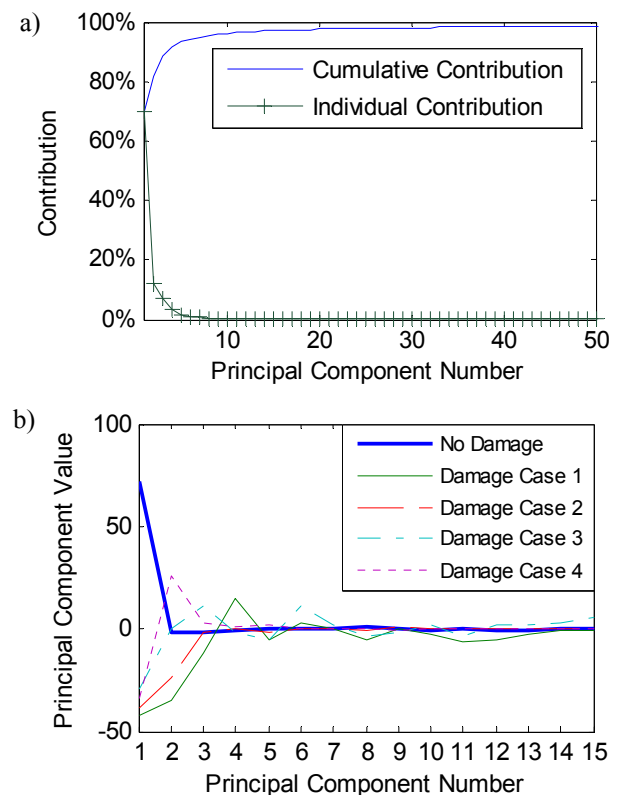


Figure 7. a) PC contributions, and b) PC values.

To ensure that at least 95% of data is represented, the first 15 PCs were considered as input to the ANN models. PCA was applied to all residual FRF data of all accelerometers. Figure 7b illustrates an example of the derived PCs of the residual FRFs. It

can be seen that the PCs of the five condition cases show unique and distinguishable features.

To enable the same data transformation for subsequent testing data sets, the eigenvalues of the covariance matrix used to define the PCs of the FRF data, and the mean and standard deviation values of each data point along the FRF are saved. Thereby, subsequent data can be converted to standard scores, making the test data compatible with the stored eigenvectors.

4.4 Artificial Neural Networks

ANNs mimic biological neural networks and use weighted interconnected processing elements called neurons to learn and map set input variables to output variables by adjusting the input weights and biases of the neuron connections according to the adjusted transfer functions. The Neural Network Toolbox in MATLAB was used to carry out the regression-type ANN analysis.

In this study, a total of 15 individual networks were trained, each with data from the 15 accelerometers, and one network ensemble, fusing the outcomes of the individual networks. For each network, the available data was divided into a training, a validation and a testing set. While each network was trained with the training samples, its performance was supervised utilizing the validation set to avoid over-fitting. The testing data was used to test the trained networks with before unseen data. All networks consisted of an input layer made up of 15 nodes representing the first 15 PCs. This was followed by a hidden layer of 7 nodes, which was followed by the output layer consisting of a single numeric node predicting the length of the damage cut. The regression-type network analysis was optimised to minimise the mean squared error of the outputs using the Levenberg-Marquardt back propagation algorithm.

4.5 TESTING THE ANN MODEL INTERPOLATION

One focus of this research was to explore the ability to train ANNs using measurements based on the healthy state and a limited number of damage cases and to test whether the trained network can accurately estimate the damage cut length from measurements of damage cases that were not used to train the ANNs.

Therefore, the available data was divided into a training and validation set, and a testing set. The training and validation set included the following cases:

- Healthy State – No Damage
- Damage Case 2 – 150 mm cut

- Damage Case 4 – 270 mm cut

Each of these three cases was divided into 100 training, 25 validation and 25 testing samples. The remaining two damage cases were used purely to test the ability of the network to interpolate between the trained cases. They are referred to as the testing cases in this study and include the following. The division of the data set is summarised in Table 2.

- Damage Case 1 – 75 mm cut
- Damage Case 3 – 225 mm cut

The training and validation sets were used to produce the eigenvectors that compressed the residual FRF data to PCs and to train/validate the ANN model. These Eigenvector features were stored and subsequently used to process the testing set after the ANN training process. In particular, the PC values from each impact excitation were generated by multiplying the previously stored Eigenvectors of the covariance matrix by the standard score of the residual FRF data points. These PCs were then used as inputs to the already trained ANN regression model to obtain the damage cut length prediction.

Table 2. Division of data for the healthy state and four damage cases into training, validation and testing set.

Damage case	Cut length (mm)	Data set division		
		100 (Train)	25 (Val)	25 (Test)
HS	0	100 (Train)	25 (Val)	25 (Test)
D1	75	150 (Test)		
D2	150	100 (Train)	25 (Val)	25 (Test)
D3	225	150 (Test)		
D4	270	100 (Train)	25 (Val)	25 (Test)

As transfer functions, the linear, logistic sigmoid and hyperbolic tangent transfer functions were studied to test the interpolation capabilities of the ANNs. Although it was necessary to optimise the ANN model to achieve a high accuracy of the cut length for the training and validation samples, consideration also needed to be given to the two damage cases in the testing set that were not used to adjust the ANN model. It was found that the logistic sigmoid and the hyperbolic tangent functions improved the overall accuracy of the ANN models for the training and validation set, however, these models were unable to provide reasonable estimates for the testing set. This suggests that the ANN model was over-trained to specifically recognise the input data that was used to train the model. The linear transfer function was also tested. It was found that, although, the training set data were not as accurately predicted, the estimations for the testing cases were much more reasonable. Hence, the linear transfer function was used for the hidden layer and the output layer in the ANN models.

An ANN ensemble was used to combine the results of the individual accelerometer ANN models and to thereby give an improved estimation of the damage cut length. The schematic of the network ensemble is shown in Figure 8.

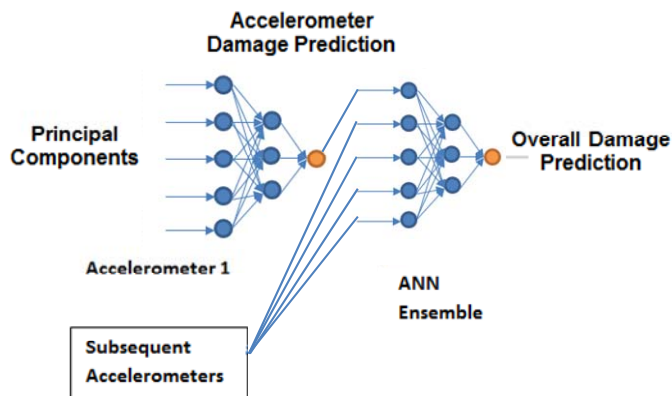


Figure 8. ANN Ensemble.

5 NUMERICAL MODELLING

A numerical model was created to simulate the experimental setup and to introduce more damage cases. The commercial software ANSYS® was used to conduct the numerical analysis of the concrete arch cantilever. The geometry of the model was based on the specimen in the experimental setup. The created model had a length of 2 m and a width of 1 m. The cross-section is shown in Figure 2b. The model consisted of two main materials, i.e. steel and concrete. The structure mostly comprised of a 32 MPa characteristic strength concrete, which was modelled using a Young's Modulus of 30.1 GPa, a Poisson's ratio of 0.2 and a density of 2.4 t/m³. The second material property used in the model is the steel I-Beam that sits along the beam axis with a 50 mm concrete cover on both ends. The steel I-Beam was modelled with a Young's Modulus of 200 GPa, a Poisson's ratio of 0.3 and a density of 7.85 t/m³.

The boundary conditions of the FE model needed to be adjusted to account for the semi-rigid supports of the experimental setup. This was achieved by modelling thin strips at the boundary conditions at three locations as indicated in Figure 9 to reflect the real experimental setup conditions. The material properties of the strips were optimised to simulate the contact between the specimen and the support.

A modal analysis was run to determine the mode shapes and natural frequencies of the structure. This was a necessary procedure, as the transient analysis was computationally expensive and the modal analysis allowed for optimisation between the experimental natural frequencies and the numerical natural frequencies. The natural frequencies of the first four

modes are listed for the experimental and numerical model in Table 3.

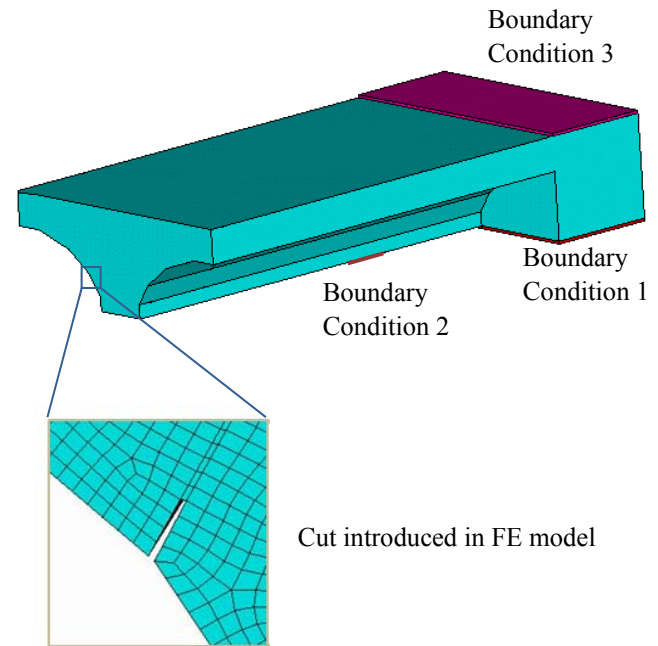


Figure 9. Finite element model with marked boundary conditions and simulated damage mesh.

Table 3. Comparison of experimental and numerical natural frequencies.

	Mode 1	Mode 2	Mode 3	Mode 4
Experimental (Hz)	45.50	180.50	263.50	400.00
FEA (Hz)	46.68	175.99	258.06	383.72
Error	2.59%	-2.50%	-2.06%	-4.07%

Transient analysis was used to obtain the time-history of the dynamic response of the structure. Therefore, a load was applied replicating the hammer impact excitation of the experimental specimen. The transient analysis produces a much cleaner signal than the experimental measurements, as it is not subjected to noise. For this reason, 2% artificial white Gaussian noise was added to the acceleration time history data. White Gaussian noise was added 150 times to each measurement in order to produce 150 unique hammer excitations to train the ANN model. Following the addition of the noise, the data was transformed into FRFs. The damage cases were produced by introducing a cut into the numerical model as shown in Figure 9. The ANNs were trained using the same procedure that was used to process the experimental data.

One of the main advantages of using numerical models is that it enables the training of ANN models with additional damage cases that can easily be produced without the need to spend extensive resources on experimental testing. In this study, a numerical model was produced to simulate the damage cases that were introduced in the experimental model. In addition, four extra damage cases were created with

the severity of the damage being midway between the existing experimental damage cases. Thereby, a total of eight different damage cases were created. The following cases were used for ANN training and validation: No Damage, 75 mm cut, 150 mm cut, 225 mm cut, 270 mm cut. To test the interpolation capabilities of the ANN model, the following damage cases were used: 37.5 mm cut, 112.5 mm cut, 187.5 mm cut and 247.5 mm cut.

For the numerical cases, the division of the data in testing, validation and training sets is summarised in Table 4.

Table 4: Division of data for the healthy state and eight damage cases into training, validation and testing sets.

Damage case	Cut length (mm)	Data set division		
		Train	Val	Test
HS	0	100 (Train)	25 (Val)	25 (Test)
D0.5	37.5	150 (Test)		
D1	75	100 (Train)	25 (Val)	25 (Test)
D1.5	112.5	150 (Test)		
D2	150	100 (Train)	25 (Val)	25 (Test)
D2.5	187.5	150 (Test)		
D3	225	100 (Train)	25 (Val)	25 (Test)
D3.5	247.5	150 (Test)		
D4	270	100 (Train)	25 (Val)	25 (Test)

6 RESULTS AND DISCUSSION

For the experimental structure, the testing set regression outcomes of the neural networks are shown in Figure 10. Figure 10a depicts the estimated damage length estimation of data from accelerometer 1, and Figure 10b shows the results of the ensemble. As mentioned above, for the testing sets, 25 samples were used from the healthy case, damage case 2 and damage case 4, and the full set of 150 samples was used from damage case 1 and damage case 3. In both figures, the regression shows smaller errors for the damage cases that were also included in the training and validation sets (healthy case, damage case 2 and damage case 4), as the networks were optimised for these particular cases. However, success can be seen in the interpolation of these results, even though a larger scatter for the tested case can be observed. This is to be expected, as the ANN model was not optimised to these cases. Furthermore, a majority of the predicted values appears to have an offset from the actual value. This suggests that training the model using only data from the healthy case, damage case 2 and damage case 4 has not accurately captured the relationship between the compressed FRF data and the actual damage cut length; however, it does give a reasonable estimate. It can be seen that

the ensemble improved the accuracy of the length estimation with an improved R value.

The numerical modelling equivalent to the experimental training and testing of the ANN was also run. The regression plots are shown in Figure 11. Similar to the experimental analysis, the numerical approach used the healthy state and damage cases 2 and 4 to train the ANN model and tested the generalisation ability of the ANN using the two damage cases that were not used in the training process.

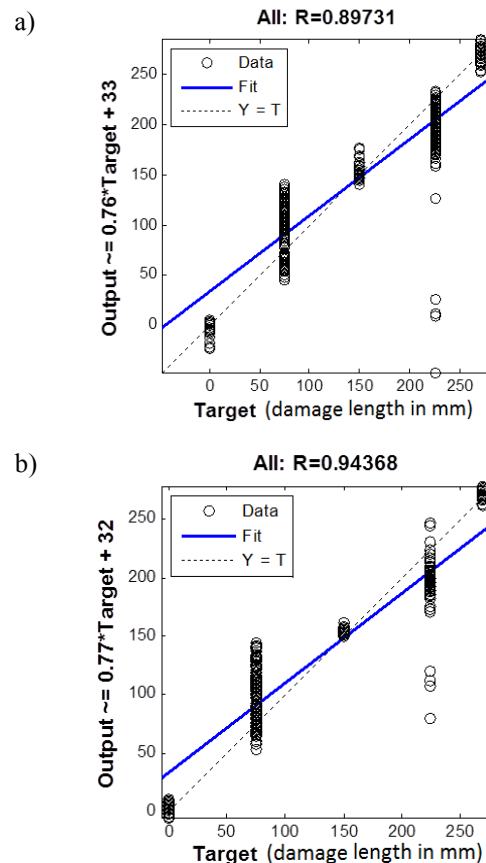


Figure 10. Experimental test regression for (a) network of accelerometer 1, and (b) network ensemble.

Despite the 2% white Gaussian noise that was added to the time history of the acceleration measurements, the regression of the estimated against the actual damage cut lengths had less scattered estimates than those of the experimental results. Again, it was found that the estimated damage lengths for the tested cases had an offset from the actual damage length, although the estimation was reasonable. The regression plot of Figure 11b shows the advantages of using a network ensemble. It can be seen that the scatter of the results was reduced, providing a clearer value as to how the ANNs have interpolated the results.

In order to improve the interpolation capabilities of the ANN, an additional numerical model was studied that introduces more damage cases to the structure. In this configuration, the healthy case and four damage cases were used to train the model and

four damage cases were used to test the interpolation capabilities of the model. Figure 12a shows the regression for a single accelerometer with the increased number of damage cases. It is evident that with the increased number of damage cases used to train the ANN model, the generalisation ability of the ANNs has been improved. This highlights the main advantages of using numerical modelling to produce data from simulated damage. Like the previous ANN setups, the ensemble has reduced the scatter of the estimated damage cut lengths showing a clearer estimation to the captured relationship between the input and output of the ANN model.

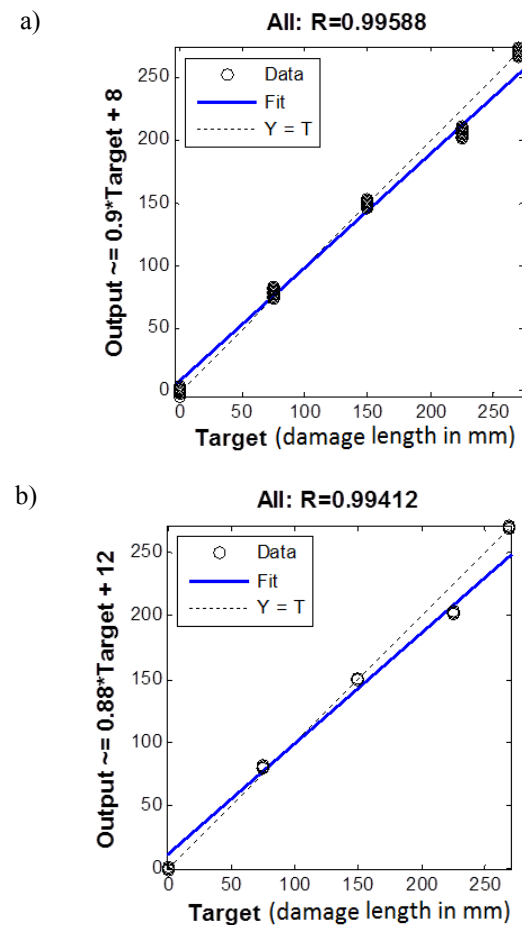


Figure 11. Finite element test regression using the same damage cases as experimental for (a) accelerometer 1 and (b) network ensemble.

Figure 13 shows the averaged values of the damage cut length estimations of each damage case for the experimental ANNs and the two numerical modelling configurations. Table 5 shows the error percentages associated with the regression plots in Figure 13. These results are to be seen as final outcomes of the proposed damage identification method.

It is observed from the chart that the average of the interpolated values do not lie perfectly with the actual damage length. In the experimental ANN configuration, the ANN model estimated the cut to be 98 mm as opposed to the actual cut length of 75 mm for damage case 1, resulting in a 31.2% error. Simi-

larly for damage case 3, the ANN model estimated the damage length to be 196 mm as opposed to the actual cut length of 225 mm, resulting in a -12.88% error.

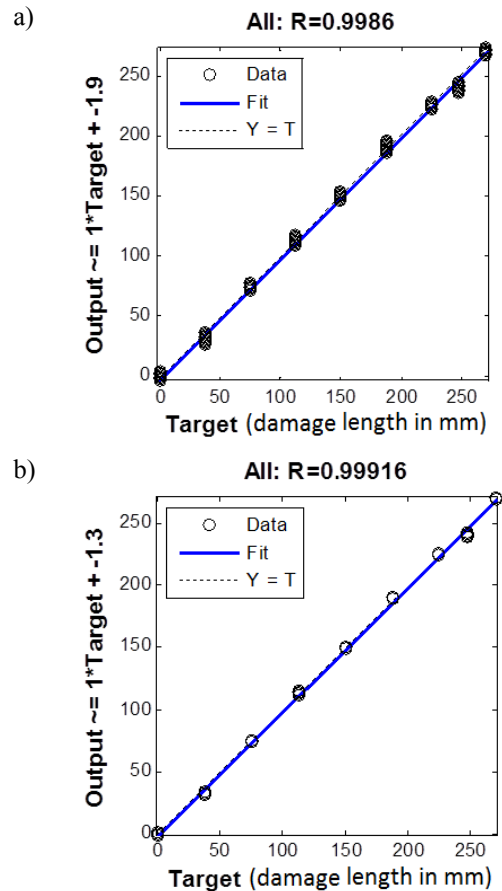


Figure 12. Finite element test regression using additional damage cases for (a) accelerometer 1 and (b) network ensemble.

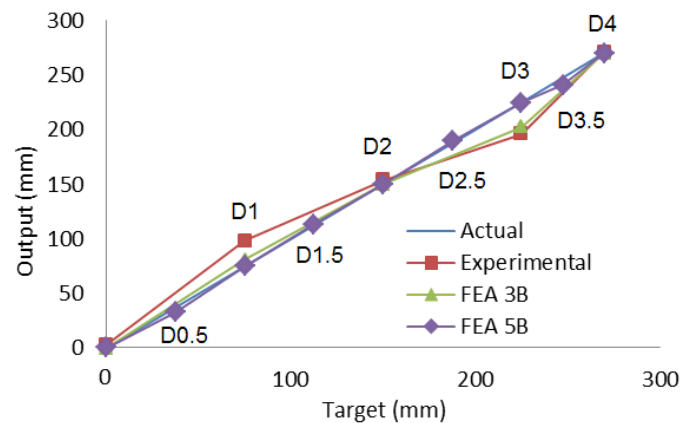


Figure 13. Averaged results of all investigated cases.

As for the numerical case with the same configuration as the experimental case, the damage length estimation for damage case 1 is much closer to the actual value than the experimental estimation with a predicted length of 81 mm and an error of 7.8%. However, the error of the predicted cut length for damage case 3 is closer to the experimental value than the actual value, suggesting that although the

networks are able to interpolate that the damage length lies in between the trained cases, it cannot accurately predict the damage length.

Table 5: Error of damage cut length of all investigated cases.

Damage case	Cut length (mm)	Experimental structure	Numerical model	Numerical model with extra cases
D0	0	-	-	-
D0.5	37.5	-	-	-12.40%
D1	75	31.20%	7.80%	-0.20%
D1.5	112.5	-	-	0.77%
D2	150	2.56%	-0.05%	0.07%
D2.5	187.5	-	-	1.15%
D3	225	-12.88%	-9.89%	-0.07%
D3.5	247.5	-	-	-2.56%
D4	270	0.42%	0.00%	0.04%

This issue can be addressed by training the networks with more cases, which can more accurately capture the relationship between the compressed FRF data and the damage cut length. It is observed from Figure 13 that interpolation improved when training more damage cases to the ANN.

In the presented study, for the experimental testing, the healthy structure and two damage cases were used to train the model. However, it was found that these three cases were not enough to capture the relationship between the compressed FRF and the damage length. In order to address this issue, numerical modelling was used to create more damage cases that could improve the ANN model's capabilities to interpret the compressed FRF data and accurately estimate the damage length accordingly. Furthermore, the results of the ANN have been combined in an ensemble to reduce the scatter of the plots and obtain higher damage identification accuracy.

7 CONCLUSIONS

This paper presents an innovative method for identifying the presence of local damage in a structure and estimating its severity. An experimental specimen that replicates a single joint of a series of jack arch beams that support the bus lane under the Sydney Harbour Bridge was used as the basis of this study. Local damage was inflicted to the specimen with four different damage severities (damage cut lengths). From impact testing, acceleration measurements were recorded for each damage case and derived to obtain residual frequency response function. These were then compressed into dimensionally smaller data size using principal component analysis. The compressed data was used to train artificial neural network models to learn the relationship be-

tween the compressed FRF measurements and the damage severity. A limited number of damage cases were used to train the networks and the remaining damage cases were used to test the models. The experimental results showed that the testing cases were able to interpolate between the trained cases using the compressed FRF data. In addition, a numerical model of the experimental structure was created to benefit from the capability of generating additional damage cases to be trained in the ANN model. From the numerical study, it was found that training the ANN models with more damage cases allows the model to better capture the relationship between the compressed FRF data and the damage severity and therefore improve the interpolation capabilities of the ANN models.

8 REFERENCES

- Bandara, R., Chan, T. and Thambiratnam, D. "Frequency response function based damage identification using principal component analysis and pattern recognition technique", *Engineering Structures*, Vol. 66, May 2014, pp. 116-128.
- Dackermann, U., Li, J. and Samali, B. "Identification of member connectivity and mass changes on a two-storey structure using frequency response functions and artificial neural networks", *Journal of Sound and Vibration*, Vol. 332, No. 16, August 2013, pp. 3636-3653.
- Dyke, S., Caicedo, J., Turan, G., Bergman, L., and Hague, S. "Phase I Benchmark Control Problem for Seismic Response of Cable-Stayed Bridges", *J Struct Eng - ASCE*, vol. 129, July 2003, pp. 857-872.
- Highway Engineering Australia "Sydney harbour bridge: 80 years on and going strong", *Highway Engineering Australia*, vol. 44, No. 3, October 2012, pp. 26-30.
- Koh, B.H. and Dyke, S.J. "Structural Health monitoring for flexible bridge structures using correlation and sensitivity of modal data", *Computers and Structures*, vol. 85, February 2007, pp. 117-130.
- Li, J., Dackermann, U., Xu, Y. and Samali, B. "Damage identification in civil engineering structures utilizing PCA-compressed residual frequency response functions and neural network ensembles", *Structural Control and Health Monitoring*, Vol. 18, No. 2, December 2009, pp. 207-226.
- Magalhães, F., Cunha, A. and Caetano, E. "Vibration based structural health monitoring of an arch bridge: From automated OMA to damage detection", *Mechanical Systems and Signal Processing*, Vol. 28, April 2012, pp. 212-228.
- Ni, Y. Q., Zhou, X. T., and Ko, J. M. "Experimental investigation of seismic damage identification using PCA-compressed frequency response functions and neural networks", *Journal of Sound and Vibration*, Vol. 290, February 2006, pp. 242-263.
- Ye, X.W., Ni, Y.Q., Wong, K.Y. and Ko, J.M. "Statistical analysis of stress spectra for fatigue life assessment of steel bridges with structural health monitoring data", *Engineering Structures*, vol. 45, December 2012, pp. 166-176.
- Zang, C. and Imregun, M. "Structural damage detection using artificial neural networks and measured FRF data reduced via principal component projection", *Journal of Sound and Vibration*, vol 242(5), May 2001, pp. 813-827.